

The First Empirical Mass Loss Law for Population II Giants¹

Livia Origlia², Robert T. Rood³, Sara Fabbri⁴, Francesco R. Ferraro⁴, Flavio Fusi Pecci²,
R. Michael Rich⁵

ABSTRACT

Using the Spitzer IRAC camera we have obtained mid-IR photometry of the red giant branch stars in the Galactic globular cluster 47 Tuc. About 100 stars show an excess of mid-infrared light above that expected from their photospheric emission. This is plausibly due to dust formation in mass flowing from these stars. This mass loss extends down to the level of the horizontal branch and increases with luminosity. The mass loss is episodic, occurring in only a fraction of stars at a given luminosity. Using a simple model and our observations we derive mass loss rates for these stars. Finally, we obtain the first empirical mass loss formula calibrated with observations of Population II stars. The dependence on luminosity of our mass loss rate is considerably shallower than the widely used Reimers Law. The results presented here are the first from our Spitzer survey of a carefully chosen sample of 17 Galactic Globular Clusters, spanning the entire metallicity range from about one hundredth up to almost solar.

Subject headings: stars: Population II, mass loss – circumstellar matter – infrared: stars

¹ This work is based on observations made with the Spitzer Space Telescope, which is operated by the Jet Propulsion Laboratory, California Institute of Technology under a contract with NASA. Support for this work was provided by NASA through an award issued by JPL/Caltech.

²INAF–Osservatorio Astronomico di Bologna, Via Ranzani 1, I-40127 Bologna, Italy, livia.origlia oabo.inaf.it, flavio.fusipecci oabo.inaf.it

³Astronomy Department, University of Virginia, Charlottesville, VA 22903, rtr virginia.edu

⁴Università degli Studi di Bologna, Dip. di Astronomia, Via Ranzani 1, I-40127 Bologna, Italy, sara.fabbri studio.unibo.it, francesco.ferraro3 unibo.it

⁵ Department of Physics and Astronomy, University of California at Los Angeles, Los Angeles, CA 90095-1547, rmr astro.ucla.edu

1. Introduction

Though the current generation of theoretical models can reasonably reproduce the general framework of stellar evolution, there are still a number of physical phenomena which are poorly understood. Among these the stellar mass loss (hereafter ML) is one of the most vexing. This is particularly the case for cool stars. Indirect evidence shows that ML strongly affects all of their late stages of evolution, yet we have little theoretical or observational guidance of how to incorporate ML into our models. We have relied on empirical laws like that of Reimers (1975a,b) based on observations of Population I giants. While subsequent work (Mullan 1978; Goldberg 1979; Judge 1991; Catelan 2000) led to slight refinements, a “Reimers Law” or some variant has been the *only* basis for stellar evolutionary models of cool stars at all ages and metallicities. Indeed, a ML law directly calibrated on Population II low-mass giants has never been determined. Galactic globular clusters (GGCs) are particularly attractive observational targets because there is so much indirect, *but quantitative*, evidence for ML. This includes the observed morphology of the horizontal branch (HB) in the cluster color-magnitude diagrams (CMDs), the pulsational properties of the RR Lyrae stars, and the absence of asymptotic giant branch (AGB) stars brighter than the red giant branch (RGB) tip, and the masses inferred for white dwarfs in GGCs (Rood 1973; Fusi Pecci & Renzini 1975, 1976; Renzini 1977; Fusi Pecci et al. 1993; D’Cruz et al. 1996; Hansen 2005; Kalirai et al. 2007).

Direct evidence for ML in GGC RGB stars has been inferred from blue shifted features of photospheric lines like $H\alpha$ (Dupree 1986; Mauas, Cacciari, Pasquini 2006). These are difficult observations and hard to convert to ML rates. One can also observe the outflowing gas much further from the star after it has formed dust. We detected this circumstellar (CS) matter using ISOCAM and were able to derive ML rates for a modest sample of RGB stars (Origlia et al. 2002). Mid-IR observations have the advantage of sampling an outflowing gas fairly far from the star (typically, tens/hundreds stellar radii). Such gas typically left the star a few decades previously, hence the inferred ML rate is also smoothed over such a timescale. From a combined physical and statistical analysis, our ISOCAM study provided ML rates and frequency. We found that *i*) the largest ML occurs near the very end of the RGB evolutionary stage and is episodic, *ii*) typical rates are in the range $10^{-7} < dM/dt < 10^{-6} M_{\odot} \text{ yr}^{-1}$, *iii*) the modulation timescales must be greater than a few decades and less than a million years, and *iv*) there is evidence for dusty shells at even the lowest metallicities. However, our ISOCAM survey suffered from two significant limitations. The small sample of observed clusters and the consequent low number of detected giants allowed us to reach only weak conclusions on the ML dependence on metallicity and HB morphology. Further, the modest spatial resolution and sensitivity compromised our ability to measure lower ML rates near the RGB tip and made it impossible to explore ML much below the RGB tip.



Fig. 1.— Three color ($3.6\mu\text{m}$ (blue), $6\mu\text{m}$ (green), $8\mu\text{m}$ (red)) mosaiced image of 47 Tuc from IRAC.

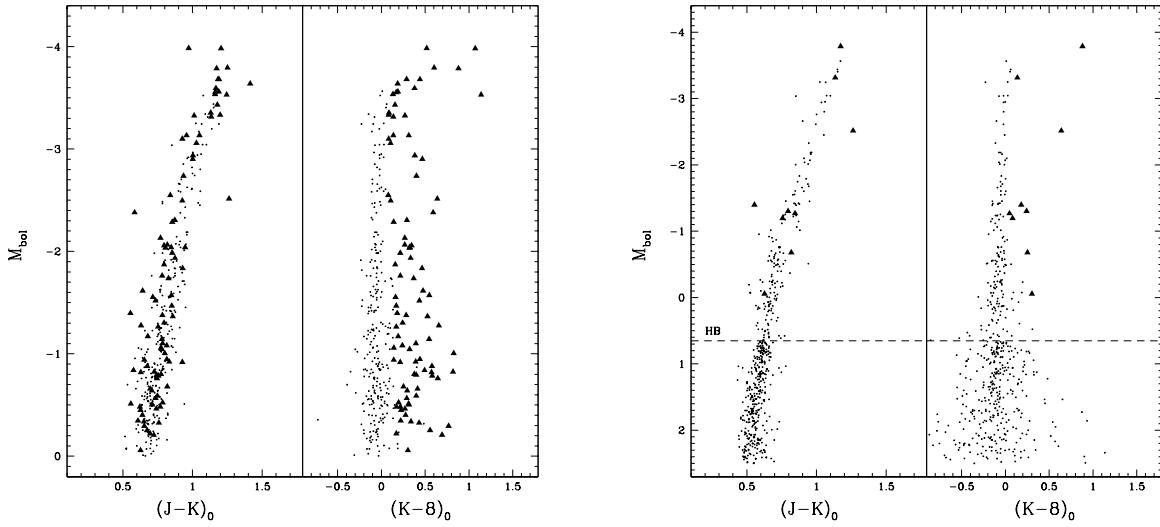


Fig. 2.— Absolute CMDs in the near IR and Spitzer planes of 47 Tuc. Left panel: stars detected in the shallow survey down to $K \approx 11$ or $M_{\text{bol}} \approx 0$ over a useful $8' \times 5'$ field of view. Right panel: stars detected in the deeper survey down to $K \approx 14$ which excludes the inner $\approx 2'$ (by radius) region. The dashed horizontal line marks the position of the HB level. Stars with $(K - 8)_0$ color excess at a 3σ level are marked as filled triangles.

2. The Spitzer IRAC survey

A sample of 17 massive GGCs, 4–5 per each 0.5 dex bin in metallicity between $[\text{Fe}/\text{H}] = -2.3$ and -0.5 and different HB morphologies within each bin has been observed with IRAC onboard Spitzer with 26 hr of observing time allocated to our program (ID #20298) in Cycle 2. For all these clusters complementary near-IR and UV photometry are available to properly characterize both the red and the blue sequences.

In this Letter we discuss the first cluster analyzed, 47 Tuc. This cluster was observed on September 21, 2005. We used a 1×3 grid with small cycling dither pattern to cover the central $9' \times 5'$ of the cluster in all the four IRAC filters and the *High Dynamic Range* Readout Mode, to avoid saturation of the brightest giants. A total observing time of 1.2 hr allowed us to reach $K \leq 14$ with $S/N \approx 20$. Fig. 1 shows the mosaiced three-color image of 47 Tuc. The Post BCD mosaic frames from the Spitzer Pipeline (Software Version: S13.2.0) have been photometrically reduced with ROMAFOT (Buonanno et al. 1983), a software package optimized for Point Spread Function fitting in crowded and undersampled stellar fields. Because of the intrinsic luminosity of 47 Tuc, the crowding in its central region is critical even at $8 \mu\text{m}$. We thus obtained two photometric catalogs: a shallow one down to $K \approx 11$ over a useful $8' \times 5'$ field of view and a deeper one down to $K \approx 14$ which excludes the inner $\approx 2'$ (by radius) region. The overall photometric uncertainty in all the four IRAC filters is ≤ 0.1 mag. Complementary ground-based near-IR photometry of the central region at high spatial resolution has been obtained using IRAC2 ESO2.2m, and SOFI ESO-NTT (Ferraro et al. 2000; Valenti et al. 2004) and supplemented with 2MASS data in the external region. The degree of completeness of the near-IR survey is 100% over the full magnitude range covered by the Spitzer survey. The shallow Spitzer catalog counts almost 400 stars and it is $\geq 86\%$ complete in the upper two RGB magnitudes, and $\approx 66\%$ complete at $0 \geq M_{\text{bol}} > -2$, while the deeper Spitzer catalog in the outer region counts almost 500 stars and it is $\geq 83\%$ complete down to $K \leq 14$.

The two Spitzer catalogs have been combined and placed onto the 2MASS astrometric system by cross-correlating the Spitzer and the ground-based near-IR surveys. The final catalog contains almost 800 stars with J , K , and Spitzer photometry in each of the four filters.

The dereddened K_0 magnitudes and $(J - K)_0$ colors have been also used to compute the stellar bolometric magnitudes and effective temperatures, by using the transformation of Montegriffo et al. (1998), reddening ($E(B - V) = 0.04$) and distance modulus ($(m - M)_0 = 13.32$) from Ferraro et al. (1999). Fig. 2 shows the absolute color-magnitude diagrams (CMDs) of 47 Tuc in the near and mid IR planes. By knowing the stellar temperature and bolometric magnitude and using a typical RGB stellar mass of $0.8\text{--}0.9 M_\odot$, we finally estimate

the stellar radius and gravity from the following equations:

$$L_{\star} = 4\pi R_{\star}^2 \times \sigma T_{\text{eff}}^4 \quad g = GM_{\star}/R_{\star}^2$$

3. Dust excess and mass loss rates

As CS dust condenses in an outflowing wind, it can be detected as a mid-IR excess. In our pilot project using ISOCAM photometry in the 10 μm window and assuming a νB_{ν} emissivity, we showed that the bulk of CS dust around the RGB tip giants typically has temperatures in the range 300–500 K. The IRAC bands between 3.6 and 8 μm can also be used to detect this warm dust when coupled with near IR photometry used to properly characterize the stellar counterpart.

In order to select candidate stars with dust excess, we define first the mean ridge lines in each of the K_0 , $(K - IRAC)_0$ CMDs to define the average color of the stars with purely photospheric emission and to determine the overall photometric errors (σ) at different magnitude bins. These $(K - IRAC)_0$ colors are $\approx 0.0 \pm 0.1$ along the entire RGB range sampled by our survey. This is in good agreement with the prediction of theoretical model atmospheres with $T_{\text{eff}} = 3500\text{--}5000$ K from the Kurucz database. Since the 8 μm IRAC band is the most sensitive to warm dust emission, stars are flagged as dusty if they show a $(K - 8)_0$ color excess $\geq n\sigma$. These stars are also the reddest in the other IRAC bands. For these stars, we also compute the pure dust emission at 8 μm , by subtracting from the the total observed flux the photospheric contribution, given by $F_8^{\text{phot}} = F_8^{\text{Vega}} \times 10^{[-0.4 \times (K - (K - 8)_{\text{phot}})]}$, where $(K - 8)_{\text{phot}}$ is the mean ridge line color without dust excess.

The number of giants with dust excess in the shallow survey of 47 Tuc is 93 at a 3σ level. In the deeper survey of the cluster outer region, no stars with dust excess have been detected below the HB level. The seven 47 Tuc stars which showed dust excess in our ISOCAM survey have been also detected by Spitzer and confirmed as dusty stars. Among the Spitzer dusty giants, four are known long period variables (V1, V4, V6, & V8 in Clement et al. (2001)) and an other 17 stars are classified as AGB stars by Beccari et al. (2006). Hence, in the following we classify the remaining 74 giants as true RGB dusty stars.

In order to obtain the ML rates we use our modified version of the DUSTY code (Ivezić, Nenkova & Elitzur 1999; Elitzur & Ivezić 2001), to compute the emerging spectrum and dust emission at the IRAC wavelengths. We adopt Kurucz model atmospheres for the heating source and for the dust a mixture of warm silicates with an average grain radius $a = 0.1 \mu\text{m}$. Slightly different choices for the latter two parameters have negligible impact in the resulting IRAC colors and mass loss rates. While radiation pressure acting on dust might

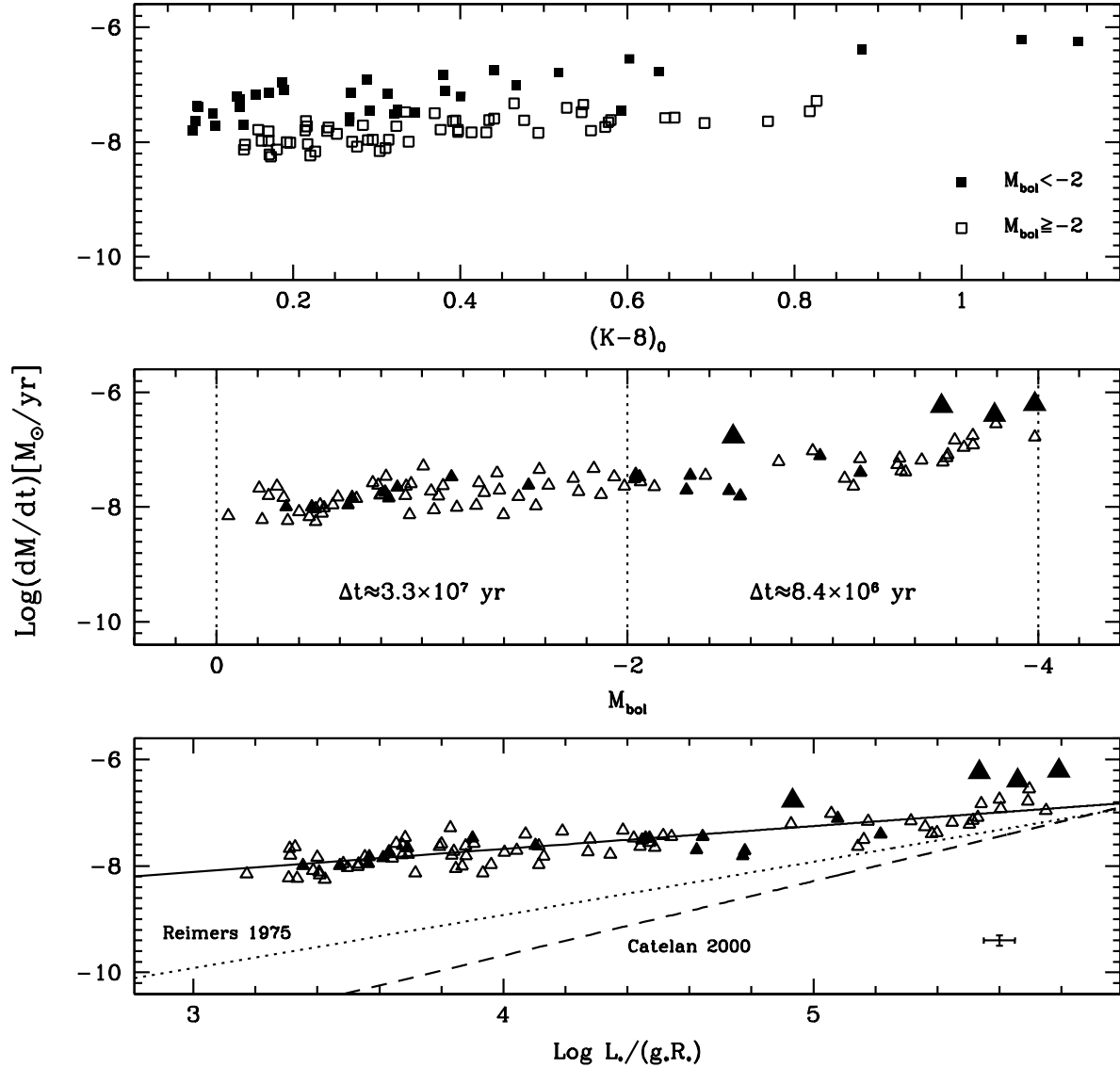


Fig. 3.— ML rates for the Spitzer sources with dust excess, as a function of the observed $(K - 8)_0$ color (top panel), bolometric magnitude (middle panel) and normalized stellar luminosity (bottom panel). In the top panel stars with $M_{\text{bol}} < -2$ and $M_{\text{bol}} \geq -2$ are plotted as filled and open squares, respectively. In the middle and lower panels filled big triangles mark those giants which are known long period variables, filled small triangles are other AGB stars. In the middle panel the evolutionary timescale Δt in 2 luminosity intervals are also reported. In the bottom panel all of the AGB stars are excluded from the fit (solid lines). Typical random error bars are shown in the bottom right corner. The empirical laws by Reimers (1975a,b) with $\eta = 0.3$ (short-dashed line) and Catelan (2000) (long-dashed line) calibrated on Population I giants are also shown for comparison.

plausibly drive winds in luminous, metal rich red giants (Willson 2000), the GGC stars are generally neither luminous nor metal rich enough for this mechanism to be efficient. Hence we run the DUSTY code under the general assumption of an expanding envelope at constant velocity v_{exp} with a density profile $\eta \propto r^{-2}$, a dust temperature for the inner boundary r_{in} of 1000 K and a shell outer boundary $r_{\text{out}} = 1000 \times r_{\text{in}}$. We then computed a large grid of DUSTY models with stellar temperatures in the 3500–5000 K range and optical depths at 8 μm (τ_8) between 10^{-5} and 10^{-1} . For each star with dust excess, we enter the grid with its empirical stellar temperature and $(K - IRAC)_0$ colors, and we exit with prediction for the optical depth, emerging flux, dust fractional contribution and envelope radius. The mass loss rates are computed by using the formula

$$dM/dt = 4\pi r_{\text{out}}^2 \times \rho_{\text{dust}} \times v_{\text{exp}} \times \delta$$

where

$$\rho_{\text{dust}} \propto \rho_g \tau_8 F_8(\text{obs}) / F_8(\text{mod}) D^2$$

is the dust density, $\rho_g = 3 \text{ g cm}^{-3}$ is the grain density, $F_8(\text{obs})$ and $F_8(\text{mod})$ are the observed and model dust emission at 8 micron, respectively, D the distance and δ the gas to dust ratio. A lower limit to δ is given by $1/Z$ where Z is the global metallicity. v_{exp} is a free parameter, which should scale like $\delta^{-0.5}$ if dust and gas are coupled. If the number of grains is increased (by decreasing δ), the momentum per grain is shared with fewer gas molecules, thus implying an enhancement of v_{exp} (Habing, Tignon & Tielens 1994; van Loon 2000). For 47 Tuc we adopt $\delta \approx 1/Z \approx 200$ and $v_{\text{exp}} = 10 \text{ km s}^{-1}$. The latter is the average expansion velocity measured in luminous, low mass giants (see e.g. Netzer & Elitzur 1993) which ranges between a few and $\approx 20 \text{ km s}^{-1}$.

4. Results and Discussion

For the dusty stars in 47 Tuc sampled by our Spitzer survey, Fig. 3 shows the inferred mass loss rates as a function of *i*) the observed $(K - 8)_0$ color, *ii*) the bolometric magnitude and *iii*) the normalized luminosity. The mass loss rate increases with increasing color excess and stellar luminosity. Also, the bulk of the mass loss along the RGB should occur above the HB level. The provisional empirical law based on such a first set of observations gives:

$$dM/dt = C \times 4 \times 10^{-10} \times (L/gR)_{\odot}^{0.4}$$

where

$$C = (\delta/200)^{0.5} \times (v_{\text{exp}}/10) \times (\rho_g/3)$$

and L_{\odot} , g_{\odot} , and R_{\odot} are the stellar luminosity, gravity and radius in solar units. In this study of 47 Tuc $C = 1$. Only true RGB stars are used to derive the fitting formula. Errors are as follows: $\approx 10\%$ for L/gR and the fit exponent and $\approx 25\%$ for the fit zero point. The latter is also a good estimate of the average random error on the final mass loss rates. As shown in Fig. 3, this new law calibrated on Population II RGB stars is significantly flatter than the original Reimers formulation and the one revised by Catelan (2000), which have slopes of 1 and 1.4, respectively.

As we found in our ISOCAM survey, only a fraction of stars along the RGB are currently losing mass: $\approx 32\%$ in the upper 2 mag, $\approx 16\%$ down to the HB. For this reason we conclude that ML is episodic. Basically mass loss is “on” for only some fraction of the time, f_{on} . By using a suitable evolutionary track for a RGB star of $M = 0.9 M_{\odot}$ and $Z = 0.004$ (Pietrinferni et al. 2006), we can derive the evolutionary timescale in each luminosity interval (see Fig. 3). Multiplying this by f_{on} , we find that the timescale ML is “on” is less than a few Myr in each interval. By using the simple equation

$$\Delta M_{\text{RGB}} = \Sigma_i (dM/dt_i \times \Delta t_i \times f_{\text{on}_i})$$

to integrate the mass loss formula multiplied by f_{on} over the RGB evolution time Δt , we find that the total mass lost on the RGB is $\Delta M_{\text{RGB}} \approx 0.23 \pm 0.07 M_{\odot}$.

In forthcoming papers we will present the results for the other clusters, with the ultimate goal of providing the first empirical ML law for Population II stars calibrated over a large range of metallicity, and investigating whether observed ML in individual stars within a cluster correlates with that cluster’s HB morphology and if ML itself is involved in the second-parameter problem.

This research was supported by the Ministero dell’Istruzione, Università e Ricerca (MIUR), the PRIN-INAF 2006 and the Italian Space Agency (ASI). RTR and RMR acknowledge support from Spitzer Science Center Grant GO-20298. We warmly thanks Elena Valenti for having provided the SOFI near IR photometric catalog and the anonymous Referee for his/her useful comments.

REFERENCES

- Beccari, G., Ferraro, F. R., Lanzoni, B., Bellazzini, M. 2006, ApJ, 652, 121
- Buonanno, R., Buscema, G., Corsi C. E., Ferraro, I., & Iannicola, G., 1983, A&A, 126, 278
- Catelan, M. 2000, ApJ, 531, 826

- Clement, C. M. 2001, *AJ*, 122, 2587
- D’Cruz, N. L., Dorman, B., Rood, R.T., O’Connell, R. W. 1996, *ApJ*, 466, 359
- Dupree, A. K. 1986, *ARA&A*, 24, 377
- Elitzur, M., & Ivezić, Z. 2001, *MNRAS*, 327, 403
- Ferraro, F.R., Messineo, M., Fusi Pecci, F., De Palo, M. A., Straniero, O., Chieffi, A., Limongi, M. 1999, *AJ*, 118, 1738
- Ferraro, F.R., Montegriffo, P., Origlia, L., Fusi Pecci, F. 2000, *AJ*, 119, 1282
- Fusi Pecci, F., & Renzini, A. 1975, *A&A*, 39, 413
- Fusi Pecci, F., & Renzini, A. 1976, *A&A*, 46, 447
- Fusi Pecci, F., et al. 1993, *AJ*, 105, 1145
- Goldberg, L. 1979, *QJRAS*, 20, 361
- Hansen, B. M. S. 2005, *ApJ*, 635, 526
- Habing, H.J., Tignon, J., & Tielens, A.G.G.M. 1994, *A&A*, 286, 523
- Kalirai, J. S. et al. 2007, *ApJ*, in press (astro-ph/07050977)
- Ivezić, Z., Nenkova, M., & Elitzur, M., 1999, *User Manual for DUSTY*, (Lexington: Univ. Kentucky)
- Judge, P.G., & Stencel, R. E. 1991, *ApJ*, 371, 357
- Mauas, P.J.D., Cacciari, C., Pasquini, L. 2006, *A&A*, 454, 609
- Montegriffo, P., Ferraro, F.R., Fusi Pecci, F., & Origlia, L. 1998, *MNRAS*, 297, 872
- Mullan, D. J. 1978, *ApJ*, 226, 151
- Netzer, N., & Elitzur, M. 1993, *ApJ*, 410, 701
- Origlia, L., Ferraro, F.R., Fusi Pecci, F., Rood, R.T. 2002, *ApJ*, 571, 458
- Reimers D. 1975a, in *Problems in Stellar Atmospheres and Envelopes*, eds. B. Baschek, W. H. Kegel, & G. Traving (Berlin: Springer), 229
- Reimers D. 1975b, in *Mem. Soc. R. Sci. Liège 6 Ser.*, 8, 369

- Renzini, A. 1977, in *Advanced Stages of Stellar Evolution*, ed. Bouvier & A. Maeder (Geneva Obs., Geneva), 151
- Rood, R.T. 1973, ApJ, 184, 815
- Pietrinferni, A. Cassisi, S., Salaris, M., Castelli, F. 2006, ApJ, 642, 797
- Valenti, E., Ferraro, F.R., Origlia, L. 2004, MNRAS, 351, 1204
- van Loon, J. T. 2000, A&A, 354, 125
- Willson, L. A. 2000, ARA&A, 38, 573